WATER RESOURCES RESEARCH, VOL. 33, NO. 7, PAGES 1669–1679, JULY 1997

Global distributions of glacier properties: A stochastic scaling paradigm

David B. Bahr[1]

Cooperative Institute for Research in Environmental Sciences, University of Colorado, Boulder

Abstract. Many problems in global climate and Earth systems science require knowledge of regional- or global-scale distributions of glacier properties, which includes mass balance, ice velocity, flux, thickness, volume, and surface area, among others. With roughly 160,000 glaciers worldwide, obtaining information on the global probability distributions of most ice properties is expensive and often infeasible. Only surface area distributions are relatively easy to measure, either by direct observation or remote sensing. While other properties are difficult to observe, this work shows that scaling relationships from the continuum dynamics of ice can link the distribution of surface areas to the global and regional distributions of any other continuum property. Some data inventories already exist for constructing reasonable distributions of glacier sizes, and this analysis presents theoretical arguments based on glacier network topologies (similar in concept to river networks) to suggest a power law times an exponential distribution of surface areas (in agreement with the data). Therefore, by using existing data or the theoretical distributions of surface areas, specific distributions for other glacier properties in any region of the world can be constructed. As an example, predictions (up to a scaling constant) are made for the distribution of glacier volumes, characteristic thicknesses, characteristic velocities, and characteristic response times in the Alps.

Introduction

As glaciers are increasingly understood to be part of a highly interdependent Earth system, a global summary of glacier properties becomes an essential component of many climate and sea level studies. Extrapolations from limited observations suggest that there are roughly 160,000 glaciers in the world, spanning in size from hundredths to thousands of square kilometers [*Meier and Bahr*, 1996]. However, with limited resources, limited time, and limited accessibility, only a few hundred of the world's glaciers (mostly in the small to midsized range) have had detailed mass balance measurements taken, and even fewer have been surveyed for velocities and other dynamical properties. Existing studies therefore can only barely cover the full range of possible glacier properties and behaviors.

Of course, one of the fundamental scientific rationales behind studying a limited number of glaciers is that many of their generic properties should be representative of all the world's glaciers. In fact, the basic continuum mechanical and hydrological properties are relatively unchanged from site to site, and given appropriate initial and boundary conditions, the general dynamics and properties of any reach of a glacier are essentially predictable. However, in many parts of the world, the size and number of glaciers are not certain, let alone their boundary conditions. With potentially tens of thousands or more small glaciers that have never been counted in surveys [*Meier and Bahr*, 1996], global and regional distributions of glacier properties simply cannot be determined from traditional continuum approaches.

A similar problem with large-scale distributions is common in hydrology. Fluid dynamics can accurately predict the flow behavior of a small reach, but entire river basins with countless branches remain beyond modeling capabilities. As a result, the discharge and other properties of a river are known to be a physical consequence of basic mass and momentum conservation, but observations of total basin discharge (and other properties) appear highly variable and essentially random. The only reasonable approach therefore has been using stochastic theories which bridge the gap between deterministic conservation principles and apparently nondeterministic large-scale processes [*Gupta and Mesa*, 1988].

For basin-scale hydrology, stochastic theories have predicted many empirically derived river "laws" and assisted, for example, in predicting the likelihood of major floods [*Singh*, 1992; *Gupta and Dawdy*, 1995]. The advantages of a stochastic-based scaling theory for glaciology would be just as relevant to many fundamental problems in modern geophysics. Consider, for example, sea level, which changes in part as a function of meltwater contributions from glaciers. Predictions of total melt cannot rely on the surface areas and volumes of measured glaciers but must account for the total distribution of surface areas and volumes for all the world's glaciers [*Meier and Bahr*, 1996]. Likewise, global albedo is a sensitive function of seasonal snow, sea ice, and land ice, but the surface areas of known glaciers give only a partial estimate. Probabilistic distributions of surface area for all the world's glaciers are necessary for a complete evaluation of global albedo. Also consider the response of ice masses to a change in climate. General circulation models (GCMs) cannot incorporate the response of a single glacier in a particular place; this is far smaller than the GCM spatial resolution. Instead, GCMs can

[1]Now at Institute of Arctic and Alpine Research, University of Colorado, Boulder.

Paper number 97WR00824.
0043-1397/97/97WR-00824$09.00

utilize the distribution of response times over large regions to give a more accurate and complete picture of the global and regional influences of climate change. Similarly, the characteristic mass balance of a single glacier is less useful to climate models than distributions of mass balance over regions comparable in size to the GCM grid cells.

The arguments for studying global and regional probability distributions can also be reversed. Not only is it better to predict distributions, but it is more meaningful to measure probability distributions in the field. Any single glacier could have aberrant behavior, uncharacteristic mass balance rates, unusual boundary conditions, or poor and unreliable data acquisition. Measurements from whole suites of glaciers, however, will indicate trends in glacier properties and behavior. Occasional outliers, measurement errors, and unaccountable randomness are expected, but regressions on distributions of glacier data identify any underlying physical consistencies.

In a break from traditional continuum mechanics, therefore, the following scaling analysis gives a theoretical foundation for manipulating global probability distributions of quantities describing the physical state of glaciers. In particular, the theory links the probability distribution of one quantity (in this case, glacier surface areas) to the global probability distribution of any other glacier property (e.g., response times, ice volumes, and flow velocities). Glacier surface areas were selected because they are an easy quantity to observe, and the global distribution of surface areas is predicted by both limited observations [*Meier and Bahr*, 1996] and geometrical scaling arguments. However, the theory is independent of the exact parameter, and if arguments can be presented for any other global distribution (e.g., velocity or ice thickness), the analysis will apply equally well. In other words, once one global distribution of some glacier property is known, the theory predicts all other global distributions.

Continuum Background and Scaling Relationships

As the following derivations demonstrate, the global probabilistic scaling theory is not independent of the continuum approach to glaciology. Instead, the global theory builds on previous studies, and its accuracy depends on a precise description of continuum properties for individual glaciers. As an example, consider the distribution of worldwide characteristic velocities. The stress equilibrium equations and constitutive relationship for ice determine flow behavior and hence every glacier's velocity field and characteristic velocity. However, a radically different constitutive law (or the same constitutive law with radically different continuum parameters, like low viscosity) would alter the velocity fields and change the predicted global distribution of characteristic velocities.

In particular, the following section will show that the relationships between different global probability distributions depend on scaling properties derived from local mass and momentum conservation (by "local" we mean separate conservation for each individual glacier). Assume, for the moment, that the global probability distribution for some glacier quantity, for example, the probability that a glacier has a given surface area, is known. Then the following analysis shows that this surface area distribution is tied to all other distributions by power laws of the form

$$[\theta] \propto [S]^p \tag{1}$$

where p is a constant, $[S]$ is a characteristic surface area, and $[\theta]$ is any other characteristic dynamical or geometrical quantity of interest (in this context, square brackets indicate a characteristic quantity). The constant p depends on the mass balance boundary conditions and parameters from the constitutive relationship of ice. The power laws follow from stretching (or scaling) symmetries of the stress equilibrium and continuity equations [*Bridgeman*, 1963; *Schmidt and Housen*, 1995; *Bahr and Rundle*, 1995].

To derive the stretching symmetries and characteristic quantities used to construct and relate global distributions, define a right-handed coordinate system with an x axis parallel to the mean surface in the direction of flow, a y axis across slope, and a z axis perpendicular to the xy plane (positive outwards). Let the x axis make an angle α with a horizontal which is perpendicular to gravity. From standard arguments of mass and momentum conservation, the continuum equations for glacier flow are

$$\frac{\partial h}{\partial t} = \dot{b} - \frac{\partial}{\partial x}\int_{h_b}^{h_s} u_x\, dz - \frac{\partial}{\partial y}\int_{h_b}^{h_s} u_y\, dz \tag{2}$$

$$\frac{\partial \sigma_{xx}}{\partial x} + \frac{\partial \sigma_{xy}}{\partial y} + \frac{\partial \sigma_{xz}}{\partial z} + \rho g_x = 0 \tag{3}$$

$$\frac{\partial \sigma_{xy}}{\partial x} + \frac{\partial \sigma_{yy}}{\partial y} + \frac{\partial \sigma_{yz}}{\partial z} + \rho g_y = 0 \tag{4}$$

$$\frac{\partial \sigma_{xz}}{\partial x} + \frac{\partial \sigma_{yz}}{\partial y} + \frac{\partial \sigma_{zz}}{\partial z} + \rho g_z = 0 \tag{5}$$

and an observationally derived isotropic constitutive law

$$\dot{\varepsilon}_{ij} = \Lambda\left(\frac{1}{2}\sum_{i,j}\sigma'_{ij}\sigma'_{ij}\right)^{(n-1)/2}\sigma'_{ij} \tag{6}$$

where i and j vary over the coordinate directions. Variables are defined in Table 1.

Following analyses by *Bahr and Rundle* [1995] and D. Bahr et al. (The physical basis of glacier volume-area scaling, submitted to *Journal of Geophysical Research*, 1996, hereinafter referred to as submission), each variable θ in (2) through (6) is rescaled (stretched) by a factor λ^r for some fixed but arbitrary constant λ and some scaling exponent r (which is different for each θ). The rescaled quantities $\lambda^r\theta$ are substituted in place of the unscaled variables of (2) through (6). By factoring λ to return to the original unscaled equations, a set of constraints on the scaling exponents r is derived. These constraints dictate the scaling relationships between characteristic values for each variable.

In particular, D. Bahr et al. (submission) find two different scaling regimes (for steep and shallow slopes) which give different sets of scaling relationships. For shallow-sloped glaciers,

$$[u_x] \propto [\Lambda][\rho]^n[|\mathbf{g}|]^n[\alpha]^n[h]^{n+1} \qquad [\dot{b}] \propto \frac{[u_x][h]}{[x]}$$

$$[\sigma'_{xz}] \propto [\rho][|\mathbf{g}|\sin(\alpha)][h]$$

$$[u_y] \propto [u_x] \qquad [\dot{b}] \propto [c_m][x]^m \qquad [\sigma_{zz}] \propto [\rho][|\mathbf{g}|\cos(\alpha)][h] \tag{7}$$

$$[t] \propto \frac{[x]}{[u_x]} \qquad [\alpha] \propto \frac{[h]}{[x]} \qquad [\sigma'_{xy}] \propto [\sigma'_{yz}] \propto [\sigma'_{xz}]$$

where m is a scaling constant determined by the longitudinal profile of the mass balance boundary condition (data suggest that $m \approx 2$ is typical (D. Bahr et al., submission)), and $[c_m] \propto [\partial \dot{b}/\partial x]$ is the "balance index" or the rate of change of $\dot{b}$ with distance x, evaluated at the equilibrium line (the elevation where $\dot{b} = 0$ on a yearly average). The steep-slope scaling relationships are identical to (7), except slope does not scale with length and thickness, so $[\alpha] \propto [h]/[x]$ is eliminated. In both cases, longitudinal gradients in stress and velocity have been neglected, and vertical stress is assumed to be hydrostatic (detailed justification of the assumptions and derivations are given by D. Bahr et al., submission).

Geometrical arguments and data from a glacier version of Hack's law for rivers (which relates basin area to channel length) suggest that characteristic glacier widths $[w]$ are proportional to characteristic glacier lengths [*Bahr and Peckham*, 1996]. Preliminary data from a Russian glacier inventory suggests that $[w] \propto [x]^{0.6}$ may be more accurate for small glaciers (work in progress). In this analysis we will assume the linear relationship, but the fundamental development of the following theory is unaltered if a nonlinear relationship proves to be more accurate (specific predictions would change slightly but not significantly, as explained below).

For a linear width-length relationship and for shallow slopes, characteristic glacier volumes and surface areas are given by

$$[V] \propto [x][w][h] \propto [x]^2[h] \tag{8}$$

and

$$[S] \propto [x][w] \propto [x]^2. \tag{9}$$

Combinations of relationships in (7) show that

$$[h] \propto [x]^{(m+n+1)/\{2(n+1)\}}. \tag{10}$$

Therefore volume is related to surface area by

$$\begin{aligned} [V] &\propto [x]^2[x]^{(m+n+1)/\{2(n+1)\}} \\ [V] &\propto ([x]^2)^{\{(m+n+1)/(4(n+1))\}+1} \\ [V] &\propto [S]^{\{(m+n+1)/(4(n+1))\}+1} \\ [V] &\propto [S]^{\gamma} \end{aligned} \tag{11}$$

where $\gamma = 11/8 = 1.375$ for typical values of $n = 3$ and $m = 2$ (parabolic mass balance profiles). Volume and surface area data for the world's small glaciers suggest an exponent of 1.36, in close agreement with this derivation [*Meier and Bahr*, 1996]. The steep-slope results are similar but with $[h] \propto [x]^{(m+1)/(n+2)}$ in place of (10). This gives a volume-area scaling exponent of $\gamma = 1.3$, slightly further from the observed value of 1.36. (A different width-length scaling exponent will slightly change the form of γ as a function of n and m. If $[w] \propto [x]^q$, then $\gamma = \{(m + n + 1)/(2(n + 1)(q + 1))\} + 1$. Similar changes would need to be made to other scaling exponents discussed in the following paragraphs, but in all cases, the modifications are trivial to derive.)

Other characteristic quantities can also be derived in terms of the surface area. For example, from (10) and (11),

$$[h] \propto [x]^{2(\gamma-1)}. \tag{12}$$

Therefore, from (9),

$$\begin{aligned} [h] &\propto ([x]^2)^{\gamma-1} \\ [h] &\propto [S]^{\gamma-1} \\ [h] &\propto [S]^{3/8} \end{aligned} \tag{13}$$

Likewise, from (7), (9), and (13),

$$\begin{aligned} [u_x] &\propto [\alpha]^n[h]^{n+1} \\ [u_x] &\propto \frac{[h]^{2n+1}}{[x]^n} \\ [u_x] &\propto \frac{[S]^{(\gamma-1)(2n+1)}}{[S]^{n/2}} \\ [u_x] &\propto [S]^{(\gamma-1)(2n+1)-n/2} \\ [u_x] &\propto [S]^{9/8} \end{aligned} \tag{14}$$

Table 2 lists a number of other power laws relating dynamical and geometrical quantities to glacier surface areas. All exponents were derived in the same manner as above, assuming shallow slopes and a linear width-length relationship. The modifications for steep slopes and nonlinear width-length relationships are trivial. (The unusual-looking negative exponents on surface slopes and response times implies that larger glaciers are less steep and that larger glaciers have a shorter response time. While seemingly backwards, this result is consistent with response time derivations in *Jóhannesson et al.*

Table 1. List of Symbols

Variable	Description
x, y, z	length along coordinate axis
w	width
h_s	surface profile
h_b	bed profile
$h = h_s - h_b$	ice thickness
V	volume
S	surface area
γ	volume-surface area exponent
α	x axis angle
ρ	density of ice
$\mathbf{g}$	gravity
$g_x = \lvert\mathbf{g}\rvert \sin \alpha$	x component of gravity
$g_y = 0$	y component of gravity
$g_z = \lvert\mathbf{g}\rvert \cos \alpha$	z component of gravity
Λ	constitutive law parameter
n	constitutive law parameter
σ_{ij}	stresses
σ'_{ij}	deviatoric stresses
$\dot{\varepsilon}_{ij}$	strain rates
u_x, u_y, u_z	components of velocity
λ, r	stretching symmetry constants
$Q \approx u_x h$	flux
t	time
$\dot{b}$	mass balance rate
m	balance rate exponent
c_m	balance index
q	width-length scaling exponent
θ, θ_t	geometric or dynamical quantity
k, k_t, κ, c, c_a	scaling constants
p, δ	scaling exponents
A	upstream basin area
ω	stream order
Ω	maximum stream order
N_ω	number of branches of order ω
A_ω	area upstream of ω
C_ω	number of links of order ω
R_N, R_A, R_C	Horton stream ratios

Symbols listed in approximate order of introduction.

Table 2. Scaling Relationships, $[\theta] \propto [S]^p$

$[\theta]$	p	p for $n = 3$, $m = 2$
$[x]$	1/2	1/2
$[w]$	1/2	1/2
$[h]$	$\gamma - 1$	3/8
$[V]$	γ	11/8
$[u_x]$	$(\gamma - 1)(2n + 1) - n/2$	9/8
$[u_y]$	$(\gamma - 1)(2n + 1) - n/2$	9/8
$[Q]$	$2(\gamma - 1)(n + 1) - n/2$	3/2
$[\sigma'_{xz}]$	$2(\gamma - 1) - 1/2$	1/4
$[\dot{b}]$	$2(\gamma - 1)(n + 1) - (n + 1)/2$	1
$[t]$	$(n + 1)/2 - (\gamma - 1)(2n + 1)$	−5/8
$[\alpha]$	$\gamma - 3/2$	−1/8

Note that $\gamma = \{(m + n + 1)/(4(n + 1))\} + 1$.

[1989] because each factor in the classical statement $[t] \propto [x]/[u_x] \propto [h]/[\dot{b}]$ has an implicit dependence on glacier length and therefore is not scale invariant. On average, the length of a glacier grows faster than its velocity, so under conditions of identical mass balance regimes (which rarely occur in nature) larger glaciers can respond faster than smaller glaciers. This is discussed in detail in a manuscript in preparation [see also *Pfeffer et al.* [1996].)

Note that from a dynamical point of view, it makes more sense to relate each quantity $[\theta]$ in Table 2 to a characteristic thickness or mass balance rather than to surface area. For example, velocity is most directly related to the thickness of a glacier (consider laminar flow solutions). However, from an observational point of view, surface area is more practical; thicknesses are difficult to observe, while surface areas are nearly trivial to measure with modern techniques of aerial photography and satellite remote sensing. As explained earlier, the choice of S is simply a matter of convenience.

Theory of Global Distributions

With the scaling relationships in Table 2, the probability distribution of any quantity $[\theta]$ can be linked to the global or regional probability distribution of glacier surface areas. *Ross* [1988] outlines the probability background necessary for the following derivations, but the fundamental concepts are simple. For monotonic functions (i.e., bijective or "single valued"), the domain of the function has a given set of values if and only if the range has another particular set of values. For example, $x^3 \in [8, 27]$ if and only if $x \in [2, 3]$. Therefore the domain of a function is greater than a given value if and only if the range is always greater than (for monotonically increasing) or always less than (for monotonically decreasing) another particular value. For example, $x^3 > 27$ if and only if $x > 3$ (monotonically increasing); and $x^{-3} > 27$ if and only if $x < 1/3$ (monotonically decreasing). In particular, characteristic glacier parameters are related to surface area by $[\theta] \propto [S]^p$. Therefore the probability that $[\theta]$ is greater than a certain value depends on the probability that $[S]$ is greater than another value (or less than another value if $p < 0$). Once the cumulative probability of $[\theta]$ is established in terms of $[S]$, a derivative will give the probability density function.

In particular, let the distribution of surface areas be given by

$$P[S = s] \equiv g(s) \tag{15}$$

for some function g, where P indicates the probability that the random variable s takes on a particular value S. (Regarding notation, for statements involving probabilities, the upper case notation will generally be used to indicate particular realizations of a lower case random variable (exceptions are p and P for scaling exponents and probability, and g and G for functions). Also note that the brackets indicating a characteristic value have been dropped to simplify notation. For example, $[S]$ is now S, and $[\Theta]$ is now Θ; square brackets with a relationship symbol inside are used to indicate a probability of that relationship.) Now let the relationship between surface area and other glacier properties be given by

$$f(s) \equiv \theta = ks^p \tag{16}$$

for some constant of proportionality, k (see appendix). As outlined above, the monotonic function f is used to relate $P[\Theta = \theta]$ to $P[S = s]$.

Assume $p > 0$. Then $\Theta \geq \theta$ if and only if $f^{-1}(\Theta) \geq f^{-1}(\theta)$, because the inverse function of f is given by $f^{-1} = (\theta/k)^{1/p}$ and is a monotonically increasing function (see (16)). Note that $f^{-1}(\Theta)$ is a particular value of the surface area, so $\Theta \geq \theta$ if and only if $S \geq f^{-1}(\theta)$. In other words,

$$P[\Theta \geq \theta] = P[S \geq f^{-1}(\theta)] \tag{17}$$

(see Figure 1a). Similarly, if $p < 0$, then f^{-1} is a monotonically decreasing function, and

$$P[\Theta \leq \theta] = P[S \geq f^{-1}(\theta)] \tag{18}$$

(see Figure 1b).

Now, to simplify notation, let $P[S \geq s] \equiv G(s)$. Then by combining equations (16), (17), and (18) and using $P[X \leq x] = 1 - P[X \geq x]$,

$$P[\Theta \geq \theta] = \begin{cases} P[S \geq (\theta/k)^{1/p}] & p > 0 \\ 1 - P[S \geq (\theta/k)^{1/p}] & p < 0 \end{cases} \tag{19}$$

$$P[\Theta \geq \theta] = \begin{cases} G((\theta/k)^{1/p}) & p > 0 \\ 1 - G((\theta/k)^{1/p}) & p < 0. \end{cases} \tag{20}$$

Therefore the distribution of values for θ is given by

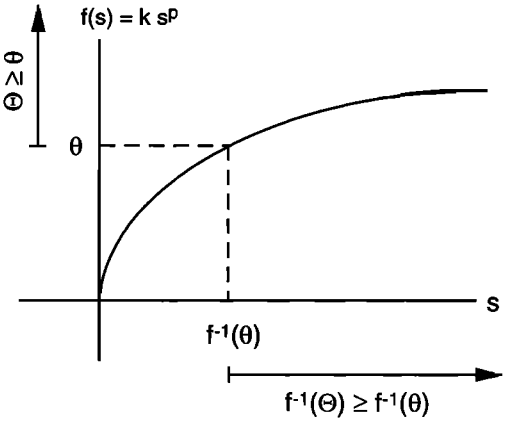

Figure 1a. A plot of $f(s) \equiv \theta \propto s^p$ for $p > 0$. Note that when a particular value of $S = f^{-1}(\Theta)$ is greater than a randomly selected $s = f^{-1}(\theta)$, then $f(S) = \Theta$ is greater than $f(s) = \theta$. In other words, $\Theta \geq \theta$ if and only if $f^{-1}(\Theta) \geq f^{-1}(\theta)$. Equation (17) is a result of this relationship.

$$P[\Theta = \theta] = -\frac{\partial}{\partial \theta} P[\Theta \geq \theta] \tag{21}$$

$$P[\Theta = \theta] = \begin{cases} -\dfrac{\partial}{\partial \theta} G((\theta/k)^{1/p}) & p > 0 \\ -\dfrac{\partial}{\partial \theta} [1 - G((\theta/k)^{1/p})] & p < 0 \end{cases} \tag{22}$$

$$P[\Theta = \theta] = \begin{cases} -\dfrac{1}{kp} (\theta/k)^{(1-p)/p} \left[\dfrac{\partial}{\partial s} G(s) \right] \Big|_{s=(\theta/k)^{1/p}} & p > 0 \\ \dfrac{1}{kp} (\theta/k)^{(1-p)/p} \left[\dfrac{\partial}{\partial s} G(s) \right] \Big|_{s=(\theta/k)^{1/p}} & p < 0. \end{cases} \tag{23}$$

Combining the two possible cases for p gives

$$P[\Theta = \theta] = -\frac{1}{k|p|} (\theta/k)^{(1-p)/p} \left[\frac{\partial}{\partial s} G(s) \right] \Big|_{s=(\theta/k)^{1/p}} \tag{24}$$

Now note that

$$\frac{\partial}{\partial s} G(s) = \frac{\partial}{\partial s} P[S \geq s]$$

$$\frac{\partial}{\partial s} G(s) = -P[S = s]$$

$$\frac{\partial}{\partial s} G(s) = -g(s). \tag{25}$$

So after substituting into (24),

$$P[\Theta = \theta] = \frac{1}{k|p|} (\theta/k)^{(1-p)/p} g((\theta/k)^{1/p}) \tag{26}$$

Equation (26) is the general form for the global distribution of any geometric or dynamical glacier quantity, θ. Note that the distribution has a remarkably simple dependence on only the power law scaling exponent p, a proportionality factor k, and the surface area distribution $g(s)$. Of these, p contains much of the interesting continuum mechanics through its relationship to the flow law exponent n (equation (6)). The role of g and k are explored in the next section, where g is shown to be another power law, and (consequently) k factors out to become trivially subsumed into a constant of proportionality. However, regardless of any specific arguments concerning the distribution of surface areas, (26) remains generally valid.

Deriving a Global Distribution

The previously outlined theory and, in particular, (26) rely on the derivation or empirical observation of at least one global distribution of a glacier quantity. This section therefore outlines the evidence for a power law distribution of glacier surface areas.

Observations

Data on the number and surface area of glaciers have been compiled by the World Glacier Inventory program [*IAHS-UNESCO*, 1989] for 35 different regions of the world. The data for each region (four of which are shown in Figure 2) show a characteristic cumulative distribution which suggests roughly a power law times an exponential tail [*Meier and Bahr*, 1996]. The departure from a simple power law or simple exponential

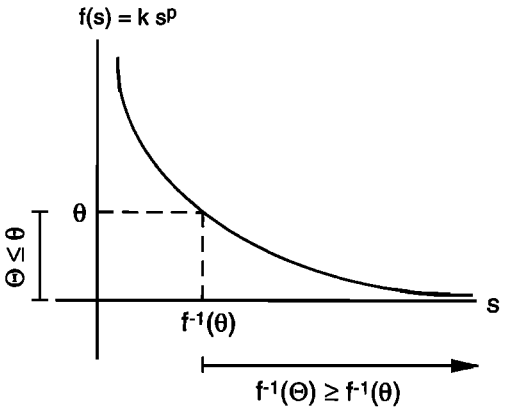

Figure 1b. A plot of $f(s) \equiv \theta \propto s^p$ for $p < 0$. Note that when a selected value of $f^{-1}(\Theta)$ is greater than $f^{-1}(\theta)$, then Θ is less than θ. This leads to (18).

distribution may be due, in part, to the paucity of data at small glacier sizes, which are often neglected in surveys. However, the data for the Alps is very comprehensive, and it still shows a power law times an exponential distribution. Only in one region with especially small glaciers (Neuquen Sur, Argentina) do the data suggest a simple power law dependence.

If a power law distribution is hypothesized for the surface area data, then both mathematically and physically, the distributions must be limited to a finite range. Probability density functions integrate to a value of 1, but integrals of power laws do not converge at one of the two limits, zero or infinity (depending on the sign of the power law exponent). Therefore, for glaciers (which decrease in frequency at increasing sizes) some other distribution must dominate as the surface area approaches zero. One possibility is that small glaciers have small characteristic thicknesses that are similar in scale to the characteristic mass balance. In that case, small glaciers are sensitive and vulnerable to seasonal, interannual, and local variability in summer melt and winter accumulation. Small glaciers will exist, but they may not survive in any one place long enough to be counted.

More importantly, though, the surface area distribution at large glacier sizes is controlled by physical boundary conditions. Glaciers cannot be larger than the region that contains them (in the extreme limit, glaciers cannot be larger than the world). Therefore the probability of getting a large glacier is skewed by the fewer possible places that could contain a large glacier. The number of large glaciers is expected to be disproportionately small relative to the number of midsized to small glaciers. This fall-off at large sizes is typical of many finite-sized systems (e.g., distributions of forest fire areas and oil field volumes [*Stauffer and Aharony*, 1991]). Typically, the finite-size effects cause the distribution to be multiplied by an exponential-like tail [*Stauffer and Aharony*, 1991], as observed in the data (Figure 2). This may, for example, explain why the Neuquen Sur data do not have an exponential tail. Unlike most of the surveyed regions, Neuquen Sur does not have any large glaciers, so the distribution cannot show any of the limiting finite-size effects.

Simple theoretical arguments also support a power law distribution of glacier surface areas with a finite-size exponential cutoff. *Meier and Bahr* [1996], for example, suggest a percolation explanation. Another explanation for surface area distri-

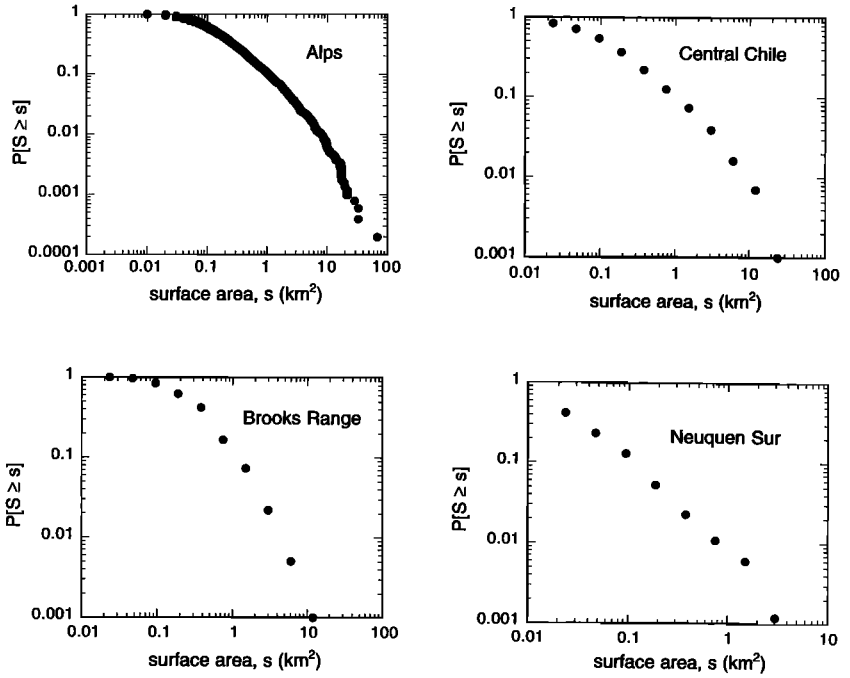

Figure 2. Empirical cumulative distribution functions for glacier surface areas in four different regions of the world. The Alps contain 5129 data points (one of the most complete surface area data sets for any region of the world), but only summary data were available for the Brooks Range (Alaska), Neuquen Sur (Argentina), and Central Chile [*IAHS-UNESCO*, 1989]. See *Meier and Bahr* [1996] for additional plots.

butions, based on some of Horton's "laws" from river geomorphology, is suggested in the following section.

A Stochastic Geometry Argument

To develop a theoretical explanation of surface area distributions, first consider the environment in which glaciers form. Glaciers typically occupy previously eroded river basins, sometimes only in the uppermost reaches, as in the Alps and Rockies, but occasionally over large portions of the basin, as in much of the Chugach Range, in Alaska. For each river basin in the world, local climate defines an equilibrium line that occurs at some elevation in the basin (in some regions, like the Appalachians, the equilibrium line may be higher than the maximum basin elevation so that no glaciers can form). Above this equilibrium line lies the accumulation area of glaciers, and below this elevation lies the ablation area and ice-free parts of the basin.

Now consider a basin selected at random from all basins in the world (or in some region) that contain glaciers. Climate is regionally and locally variable, and basins occupy many different elevation ranges, so the equilibrium line will fall at some apparently random location in the selected basin. If we assume that the accumulation area of a glacier is proportional to the area of the basin upstream from the glacier's equilibrium line (a visual inspection of basins containing glaciers suggests that this is reasonable), then the size of the glacier accumulation area will be dictated by the size of the upstream basin area. The equilibrium-line position in a basin was selected randomly, so when repeated many times (e.g., once for each basin containing a glacier), the resulting size distribution of glacier accumulation areas must be approximated by the distribution of all possible upstream basin areas.

In general, the accumulation area is roughly two thirds of the total glacier area [*Meier and Post*, 1962], so the distribution of glacier areas is the same as the distribution of accumulation areas, but stretched by a factor of 3/2. As noted above, the upstream basin areas are equivalent (up to a scalar constant) to the accumulation areas. In other words, if A is the upstream basin area, then $P[S = s] = P[A = 2/3c_a s]$ for some scalar, c_a. So the distribution of glacier areas is reduced to finding the distribution of basin areas, $P[A = a]$ (where $a = 2/3c_a s$).

Basin area distributions can be derived from a well-established empirical law which relates the area upstream of a river segment to a measure of the importance of the segment as a major or minor tributary of the entire basin. Consider a river basin as a "tree" with each branch defined by a tributary (Figure 3). The outlet of the basin is the "trunk," and the outermost branches are the "leaves." Branches (tributaries)

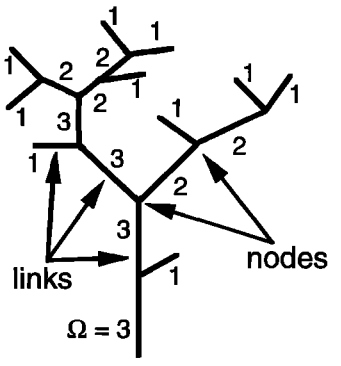

Figure 3. Hypothetical river basin with multiple tributaries. Each branch is assigned a number according to the Horton-Strahler stream-ordering scheme.

join together at points called nodes, and any section of a branch between two nodes is called a link; each branch can have many links. The Horton-Strahler stream ordering (used to rank the importance of tributaries) assigns each leaf of the tree a ranking, or stream order, ω, of 1. If these outermost leaves of order 1 are then pruned away, the remaining tree has a new set of outermost branches each of which is assigned a stream order of $\omega = 2$. The pruning and labeling process is repeated until no further branches remain, and the trunk has been assigned the largest stream order, $\omega = \Omega$ (Figure 3). (Additional details of the Horton-Strahler stream ordering are given by *Strahler* [1957]; an application to glaciers is given by *Bahr and Peckham* [1996].)

Using the Horton-Strahler stream ordering, let N_w be the number of branches of order ω (e.g., $N_3 = 1$ in Figure 3), let A_ω be the area upstream from a single branch of order ω, and let C_ω be the number of links in a single branch of order ω (e.g., $C_3 = 4$ in Figure 3). Empirical observations known collectively as Horton's laws [*Horton*, 1945] show that

$$N_\omega \propto R_N^{\Omega-\omega} \tag{27}$$

$$\langle A_\omega \rangle \propto R_A^\omega \tag{28}$$

$$\langle C_\omega \rangle \propto R_C^\omega \tag{29}$$

where R_N, R_A, and R_C are constants, and $\langle\ \rangle$ indicates the mean of a distribution (note that there is only one value for each N_ω).

In the derivations that follow, Horton's laws are combined to give the distribution of upstream basin areas and hence glacier sizes. The approach is similar to the inverse function approach used to derive the global probability distributions (equations (15) through (26)). In particular, Horton's law relates stream orders to upstream areas with a bijective function (equation (28)). This function is inverted to link (1) the probability that upstream areas are greater than a given value to (2) the probability that stream orders are greater than another value. By using (27) and (29), this is then converted to a power law expression involving only R_C, R_A, and R_N.

First, assume that each branch has an upstream area equal to the average upstream area of all other branches with the same stream order. In other words, assume the random variable $A_\omega \approx \langle A_\omega \rangle$. Also assume $C_\omega \approx \langle C_\omega \rangle$. (These are reasonable low-order approximations, although more general derivations may be possible with the full distribution of upstream areas, potentially using distributions from strong statistical self-similarity discussed by *Bahr and Peckham* [1996]. However, as with many mean field approximations in statistical mechanics, the behavior of the average upstream area is sufficient to theoretically motivate and to capture the salient features of the distribution of glacier sizes.) Define $f(\omega) \equiv \langle A_\omega \rangle = cR_A^\omega$. Then $f^{-1}(\langle A_\omega \rangle) = (\log \langle A_\omega \rangle - \log c)/\log R_A$, and by the same motivation as (17),

$$P[A \geq \langle A_\omega \rangle] = P[W \geq f^{-1}(\langle A_\omega \rangle)] \tag{30}$$

where W is a particular value of the random variable ω.

Next, consider a derivation of $P[W \geq \omega]$, modified here from a description first given by *de Vries et al.* [1994] and also by *Peckham* [1995]. Note that $N_\omega C_\omega$ is the total number of links which are in branches of order ω, and $\sum_{\omega=1}^{\Omega} N_\omega C_\omega$ is the total number of links in the entire basin. Therefore the probability that an arbitrary link in the basin has order ω is given by

$$\cdot P[W = \omega] = \frac{N_\omega C_\omega}{\sum_{\omega=1}^{\Omega} N_\omega C_\omega}. \tag{31}$$

By substituting (27) and (29) into (31) (and using the assumption that $C_\omega \approx \langle C_\omega \rangle$),

$$P[W \geq \omega] = (R_C/R_N)^{\omega-1}. \tag{32}$$

Now the derivation of upstream areas continues by combining (30) and (32) to give

$$P[A \geq \langle A_\omega \rangle] = P[W \geq (\log \langle A_\omega \rangle - \log c)/\log R_A] \tag{22}$$

$$P[A \geq \langle A_\omega \rangle] = \left(\frac{R_C}{R_N}\right)^{\{(\log \langle A_\omega \rangle - \log c)/(\log R_A)\}-1}.$$

By straightforward algebra, (33) reduces to

$$P[A \geq \langle A_\omega \rangle] = \kappa \langle A_\omega \rangle^{-\delta} \tag{34}$$

where

$$\kappa = \left(\frac{R_N}{R_C}\right) \exp\left[\frac{\log (R_N/R_C) \log c}{\log R_A}\right]$$

and

$$\delta = \frac{-\log (R_N/R_C)}{\log R_A}.$$

By assumption, $A_\omega \approx \langle A_\omega \rangle$, so $P[A \geq \langle A_\omega \rangle] \approx P[A \geq A_\omega]$. Also, (34) is independent of ω. Therefore the distribution of stream areas is given by

$$P[A \geq a] = \kappa a^{-\delta}. \tag{35}$$

To convert the distribution of upstream basin areas to glacier areas, recall that $P[S = s] = P[A = 2/3c_a s]$. Therefore the theoretical arguments based on Horton's laws predict a power law glacier surface area distribution of

$$P[S \geq s] = P[A \geq 2/3c_a s] = \kappa(2/3c_a s)^{-\delta}. \tag{36}$$

Horton's laws and the power law upstream area distributions are observed for both river basins [*Peckham*, 1995] and basins containing glaciers [*Bahr and Peckham*, 1996]. In agreement with the glacier size observations, the observations of upstream area distributions also show a finite-size cutoff at large areas [*Peckham*, 1995, pg. 107]. In other words, very few large upstream areas can fit into a finite-sized basin, just as large glaciers cannot fit into small basins.

For glacier size distributions, the finite-size effect is particularly pronounced because the equilibrium line altitude is not completely random, as assumed above. In reality, the equilibrium line is more likely to fall at higher elevations so that the upstream areas are smaller than would be possible if the equilibrium line fell at lower elevations. Therefore large glaciers are even less likely to exist in these smaller upstream areas, and the power law distribution will be multiplied by the finite-size decreasing exponential tail, as described in the previous section. However, the fundamental distribution is still power law in form. If mountain ranges had significantly greater relief with equilibrium lines at comparatively lower elevations, then bigger glaciers would not push the finite-size boundary and the power law relationship would hold over a greater range.

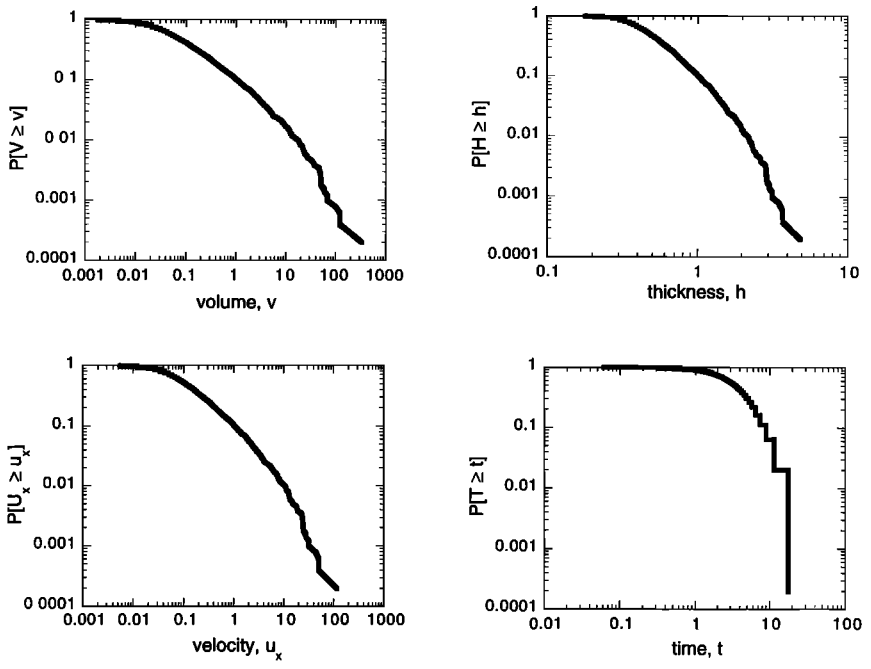

Figure 4. Predicted cumulative distributions for characteristic ice thickness, volume, velocity, and response time in the Alps. Each plot contains processed surface area information from 5129 different glaciers. Units are not given because predictions are valid only up to a rescaling of the x axis.

Predictions

Recall that the distribution of any glacier property depends on the form of the surface area distribution, $g(s)$, in (26). Although some aspects of the data collection may be flawed [*Meier and Bahr*, 1996], the preceding section suggests that the power law times exponential behavior of the glacier size data in Figure 2 is reasonable. The Alps have been studied extensively, and size data from this region are probably among the most complete. Assuming therefore that the data from the Alps are representative of actual surface area distributions, (19) and (26) can be used to predict the distributions of other glacier properties in the Alps. The technique outlined below could also be used to predict distributions in any other part of the world.

Consider the ordinate and abscissa of the ith data point in the surface area distribution, $(s_i, P[S = s_i])$. By substituting (16) and (26), this data point is related to a point on the distribution of another property θ by

$$(\theta_i, P[\Theta = \theta_i]) = (ks_i^p, (1/k)(1/|p|)s_i^{1-p}P[S = s_i]). \quad (37)$$

Similarly, by using (16) and (19), each data point on the cumulative distribution of S gives a point on the cumulative distribution of θ,

$$(\theta_i, P[\Theta \geq \theta_i]) = \begin{cases} (ks_i^p, P[S \geq s_i]) & p > 0 \\ (ks_i^p, 1 - P[S \geq s_i]) & p < 0 \end{cases} \quad (38)$$

The form of the cumulative distribution is simpler, and cumulative distributions are less noisy than density functions, so we will use (38) rather than (37) to examine distributions for the Alps.

First note that on the right-hand side of (38), s_i and $P[S \geq s_i]$ are known from data, but the constant k is unknown. However, k's only role in the cumulative distribution is to stretch the θ axis. Therefore the shape of the cumulative distribution is predicted by the rescaled equations

$$(\theta_i/k, P[\Theta \geq \theta_i]) = \begin{cases} (s_i^p, P[S \geq s_i]) & p > 0 \\ (s_i^p, 1 - P[S \geq s_i]) & p < 0 \end{cases} \quad (39)$$

In other words, by using surface area distribution data, the distribution of any property θ is predicted up to a constant scaling factor by (39).

The empirical cumulative distribution function (CDF) for glacier sizes in the Alps contains 5129 data points (Figure 2). These data were substituted into (39) to predict four different properties: characteristic ice thickness, volume, velocity, and response time. Values for p were taken from the last column of Table 2 (so linear width-length scaling and shallow slope scaling have been assumed, but again, these assumptions could be easily changed). The predicted shape of the CDFs of these four properties are shown in Figure 4.

The actual distributions of the characteristic thickness, volume, velocity, and response time must rescale (by the factor k) to the shapes in Figure 4. A regression on available data for glacier volumes and surface areas in the Alps [*Meier and Bahr*, 1996] suggests $k \approx 0.03$ (for the predicted volume CDF). However, the approximately 20 available data points undersample small glaciers relative to medium-sized glaciers and cannot be used to construct an empirical volume CDF. Unfortunately, appropriate data are also not available for comparisons to the other predictions of thickness, velocity, and response time. Future data collection strategies emphasizing area, volume, thickness, and velocity measurements over a broad range of glacier sizes would be useful for constructing empirical CDFs and testing the predicted distributions.

Sources of Error in Predictions

Predictions of distributions of any glacier property rely on the accuracy of the glacier surface area distributions. In general, the empirical CDFs of glacier size are insensitive to errors in the measured area of individual glaciers (particularly when the sample size is large, as in the Alps). However, any errors are exponentiated by p in (37) and (38). From Table 2, typical values of p are close to 1, so small errors should not increase dramatically. In some cases, like characteristic stress and thickness, p is closer to zero and errors in glacier size would be insignificant.

Many data collections undersample and hence underrepresent small or large glaciers. Constructing a proper empirical distribution requires a sampling procedure which selects a random subset of glaciers from the set of all glaciers. For example, if there are orders of magnitude more small glaciers than large glaciers, any representative subsample must also include orders of magnitude more small glaciers. Besides occasionally exhaustive measurements of surface areas (as in the Alps), data are seldom collected in representative distributions.

The effect of undersampling is illustrated in Figure 5a, where it is easy to see that the empirical CDFs change dramatically when large or small glaciers are neglected. Undersampling large glaciers, for instance, makes it seem less probable that there are glaciers greater than a given size. This causes $P[S \geq s]$ to fall off too rapidly. On the other hand, if a complete data set is subsampled randomly, as in Figure 5b, the distributions remain nearly identical.

Notice that relatively small data sets are acceptable as long as the measurements properly sample the entire range of glacier sizes. This underscores the importance of having a theoretical justification for the observed power law and exponential distributions of surface areas. Without the theory, it is difficult to know if limited observations have properly represented the extremes. However, remotely sensed information (for example, from the new Global Land Ice Monitoring from Space Project using the upcoming Advanced Spaceborne Thermal Emission and Reflection Radiometer instrument [*Kargel and Keiffer*, 1995]) is probably the best way to insure reasonable samples. Remotely sensed measurements can be automated for relatively complete and unbiased compilations of glacier surface areas as well as surface velocities [*Scambos et al.*, 1992]. Note that the resulting surface velocity distribution could be used to test predictions based on the remotely sensed surface area measurements.

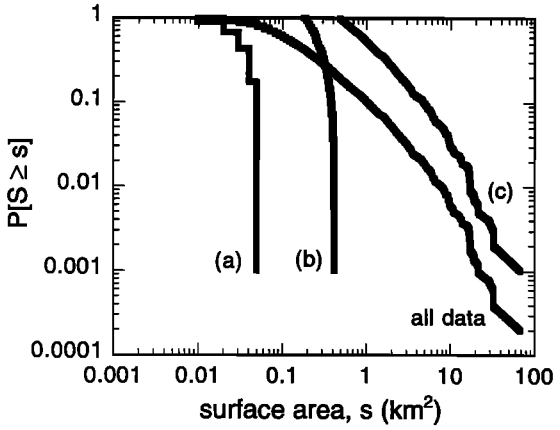

Figure 5a. A comparison of empirical CDFs of surface areas from the Alps. The plot containing all available data uses 5129 glaciers. The three subsampled distributions contain (a) the smallest 1000 of all the glaciers, (b) those midsized glaciers that are between the 3000th to the 4000th largest, and (c) the largest 1000 of the glaciers. Subsample (c), in particular, is typical of the bias in real glacier inventories, which often ignore small glaciers.

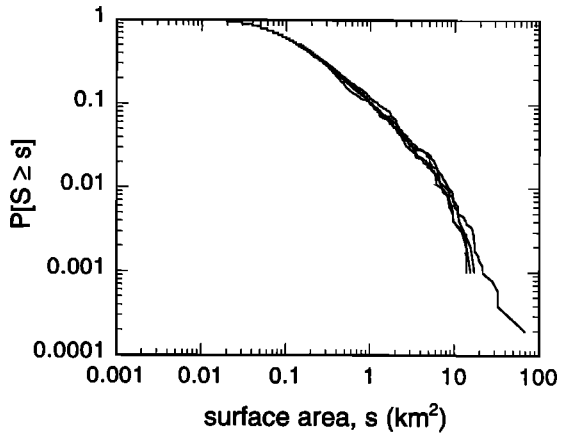

Figure 5b. A comparison of the distribution of all measured glacier sizes in the Alps to distributions which contain a random uniform subset of all the glaciers. Each of the three subsets contains 1000 of the total 5129 glaciers. The random unbiased subsets give the same empirical CDFs as the full data, unlike the biased subsets in Figure 5a.

Conclusions

The global probabilistic scaling theory is robust to perturbations in the details of the derivation. If, for example, additional data support the steep-slope rather than shallow-slope scaling, then the power laws in Table 2 will change, but the fundamental structure of the theory will remain unaltered. Similarly, changes in the width-to-length relationship (equation (8)) or constitutive law (equation (6)) will alter the scaling relationships but not the underlying theory of distributions. The probabilistic scaling theory has been constructed as a general stochastic approach to glaciology and is designed to serve as a tool for further exploration. The scaling theory is not an end in itself but provides a meaningful link between smaller-scale glacier dynamics and larger-scale regional and global behavior.

Using available data, for example, specific predictions have been made (up to a scaling constant) for the regional scale distribution of characteristic ice volumes, thicknesses, velocities, and response times in the Alps. Predictions like these can be done in many other parts of the world, particularly as remotely sensed surface area data become available. More and better glacier data on characteristic surface areas, thicknesses, velocities, etc., should be collected (in at least one region of the world) so that the scaling constants (k) in these predictions can be estimated more accurately. Then, as predictions are completed and evaluated for each region of the world, the theory will give an especially practical technique for scaling up local snow and ice data to the larger scales necessary for GCM simulations. Such a scaling link has been an outstanding problem for GCM parameterizations and a long-term goal for many Arctic systems science studies [*ARCSS*, 1991].

In addition to GCM applications, the global distributions are also a particularly attractive way to track and estimate the impact of changing climate. As surface area distributions are altered with time, the dynamical response of the world's ice masses can be easily estimated. The change can be linked potentially to shifts in mass balance distributions, and, for example, the change in volume distributions can be used to estimate changing meltwater contributions to rising sea level.

In summary, the theory takes locally valid statements of mass and momentum conservation and derives scaling relationships between continuum parameters and glacier surface areas. These scaling relationships then link the global and regional distributions of surface area to global and regional distributions of all other continuum properties. Observations suggest that large-scale distributions of surface areas have a power law times an exponential form, and derivations based on stochastic theories of basin-scale hydrology also predict a power law form with a finite-size cutoff. The theory predicts, then, that distributions of all glacier properties should have similar power law and exponential structures (equation (26)).

Note, finally, that generalizations of this stochastic scaling theory could also be used to explain the regional and global distributions of properties of other discrete weakly coupled dynamical objects in Earth systems science. The primary requirements are (1) a set of equations linking pertinent variables on local or small scales that can be rescaled to identify power law relationships between characteristic quantities and (2) a known distribution at larger scales of at least one characteristic quantity. These requirements, for example, can likely be established for snow avalanches, rock glaciers, debris flows, some aspects of river and flood dynamics, and potentially (when suitably decoupled by long time intervals) for distributions of properties of atmospheric phenomena like hurricanes.

Appendix: A Note on Different Constants of Proportionality

The constants of proportionality for the power laws in Table 2 can vary from glacier to glacier. Intuitively, this is because each glacier can have a different set of nondimensional numbers associated with its dynamics. None of the relationships in Table 2 are nondimensional, but combinations of the power laws will give nonlinear analogs to the classic nondimensional numbers for a linear viscous fluid [*Bahr and Rundle*, 1995; *Schmidt and Housen*, 1995; *Bridgeman*, 1963]. These nondimensional numbers therefore are in part a function of the constants of proportionality. So changing the nondimensional numbers (equivalent to changing the glacier flow scenario) can change the constants.

Technically, therefore, (16) should be revised to read $\theta = k_i S^p$ for the ith glacier out of the set of all glaciers. However, the scaling theory is concerned with trends in the relationships between θ and S, and the trends are not altered by the different k_i. In particular, relative to the range of possible values in S, k_i is expected to have a relatively small range of values because most glaciers have roughly similar flow regimes. Consider for example, the range of observed glacier flow behaviors (all laminar) relative to the range of observed behaviors for flowing water (laminar to turbulent). Intuitively each glacier's pertinent nondimensional numbers are different but similar, so the variation in k_i is expected to be small relative to variations in other glacier parameters like the surface area. Therefore the relationship between θ and S^p should be well-approximated by a single average constant of proportionality, $k = \langle k_i \rangle$.

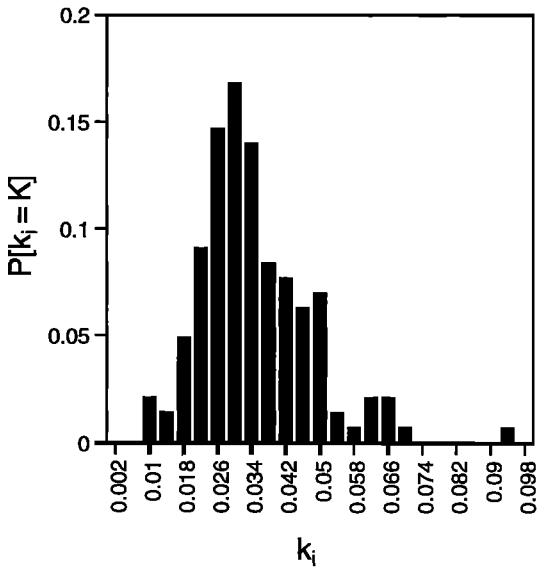

Figure 6a. A binned probability density function for k_i, derived from volume and surface area data for 144 glaciers around the world with the assumption that $p = 1.375$ (D. Bahr et al., submission). The mean of the distribution is 0.034, and the standard deviation is 0.013.

Volume and surface area data support the idea that k_i can be approximated by a well-defined average. Figures 6a and 6b show that there is a distribution of values for the constant of proportionality but that there is a clear peak at the mean value. The variability in k_i (between roughly 0.01 and 0.1) is 4 orders of magnitude less than the variability in S (between 0.1 and 10000 km^2).

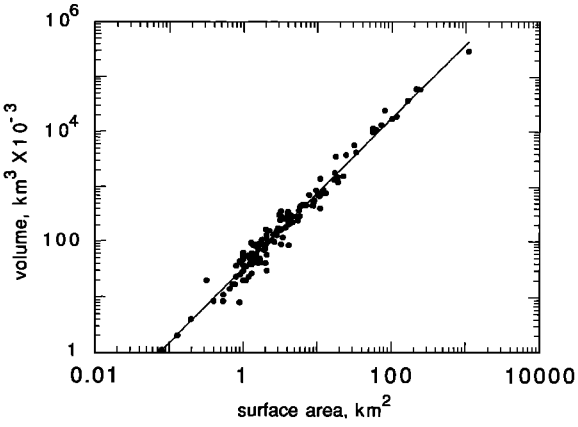

Figure 6b. A plot of log V versus log S shows visually that the variability due to k_i is small relative to the ranges of V and S. The linear fit has a slope of 1.36 (compare to the theoretical value of 1.375 in Table 2) and a squared correlation coefficient of $R^2 = 0.99$.

Acknowledgments. Special thanks to Garry Clarke, Andrew Fountain, and Ed Waddington, whose helpful reviews clarified many points in the text.

References

ARCSS, *Arctic System Science, Land/Atmosphere/Ice Interactions: A Plan for Action*, edited by L. L. McCauley and M. F. Meier, Fairbanks, Ala., 1991.

Bahr, D. B., and S. D. Peckham, Observations and analysis of self-similar branching topology in glacier networks, *J. Geophys. Res.*, *101*, 25,511–25,522, 1996.

Bahr, D. B., and J. B. Rundle, Theory of lattice Boltzmann simulations of glacier flow, *J. Glaciol.*, *41*, 634–640, 1995.

Bridgeman, P. W., *Dimensional Analysis*, Yale Univ. Press, New Haven, Conn., 1963.

de Vries, H., T. Becker, and B. Eckhardt, Power law distribution of discharge in ideal networks, *Water Resour. Res.*, *30*, 3541, 1994.

Gupta, V. J., and D. R. Dawdy, Physical interpretations of regional variations in the scaling exponents of flood quantiles, *Hydrol. Process.*, *9*, 347–361, 1995.

Gupta, V. J., and O. J. Mesa, Runoff generation and hydrologic response via channel network geomorphology—recent progress and open problems, *J. Hydrol.*, *102*, 3–28, 1988.

Horton, R. E., Erosional development of streams and their drainage basins: Hydrophysical approach to quantitative morphology, *Geol. Soc. Am. Bull.*, *56*, 275–370, 1945.

IAHS-UNESCO, *Glacier Mass Balance Bulletin, Bull. 3 (1992–1993)*, edited by W. Haeberli, E. Heeren, and M. Hoelzle, Zurich, 1994.

Jóhannesson, T., C. Raymond, and E. Waddington, Time-scale for adjustment of glaciers to changes in mass balance, *J. Glaciol.*, *35*, 355–369, 1989.

Kargel, J. S., and H. H. Kieffer, Opportunity for nearly comprehensive global glacier monitoring with ASTER, *Eos Trans. AGU*, *76*(46), 91, Fall Meet. Suppl., 1995.

Meier, M. F., and D. B. Bahr, Counting glaciers: Use of scaling methods to estimate the number and size distribution of the glaciers of the world, in *Glaciers, Ice Sheets and Volcanoes: A Tribute to Mark F. Meier*, edited by S. Colbeck, *CRREL Spec. Rep.*, *96-27*, pp. 89–94, Cold Reg. Res. and Eng. Lab., Hanover, N. H., 1996.

Meier, M. F., and A. S. Post, Recent variations in mass net budgets of glaciers in western North America, *IASH Publ. 58*, 63–77, 1962.

Peckham, S. D., Self-similarity in the three-dimensional geometry and dynamics of large river basins, Ph.D. dissertation, 286 pp., Univ. of Colo., Boulder, 1995.

Pfeffer, W. T., D. B. Bahr, and M. F. Meier, Volume-area scaling and glacier response times, *Eos Trans. AGU*, *77*(46), Fall Meet. Suppl., 182, 1996.

Ross, S., *A First Course in Probability*, 3rd ed., 420 pp., Macmillan, New York, 1988.

Scambos, T. A., M. J. Dutkiewicz, and J. C. Wilson, Application of image cross-correlation to the measurement of glacier velocity using satellite Image data, *Remote Sens. Environ.*, *42*, 177–186, 1992.

Schmidt, R., and K. Housen, Problem solving with dimensional analysis, *Ind. Phys.*, *1*(1), 21–24, 1995.

Singh, V. P., *Elementary Hydrology*, 973 pp., Prentice Hall, Englewood Cliffs, N. J., 1992.

Stauffer, D., and A. Aharony, *Introduction to Percolation Theory*, 2nd ed., 181 pp., Taylor and Francis, Bristol, Pa., 1991.

Strahler, A. N., Quantitative analysis of watershed geomorphology, *Eos Trans. AGU*, *38*, 913–920, 1957.

D. B. Bahr, INSTAAR, 1560 30th St., Campus Box 450, Boulder, CO 80309-0450. (e-mail: david.bahr@colorado.edu)

(Received October 11, 1996; revised March 7, 1997;
accepted March 17, 1997.)